Separation Science and Technology
Publication details, including instructions for authors and subscription information:
http://www.informaworld.com/smpp/title~content=t713708471

Dimensional Analysis of Crossflow Microfiltration Data

Greg Foley[a]
[a] School of Biotechnology and National Institute for Cellular Biotechnology, Dublin City University, Dubline, Ireland

To cite this Article Foley, Greg(2006) 'Dimensional Analysis of Crossflow Microfiltration Data', Separation Science and Technology, 41: 14, 3169 — 3185
To link to this Article: DOI: 10.1080/01496390600894830
URL: http://dx.doi.org/10.1080/01496390600894830

Separation Science and Technology, 41: 3169–3185, 2006

ISSN 0149-6395 print/1520-5754 online
DOI: 10.1080/01496390600894830

Dimensional Analysis of Crossflow Microfiltration Data

Greg Foley
School of Biotechnology and National Institute for Cellular Biotechnology, Dublin City University, Dubline, Ireland

Abstract: A new approach to correlating crossflow microfiltration (CFMF) data based on dimensional analysis is presented. The steady state flux was assumed to be a function of the trans-membrane pressure (ΔP), the crossflow velocity (u), the particle concentration (c), filtrate viscosity (μ), and membrane resistance (R_m). Correlations of the form $J/u = K(\Delta P/cu^2)^a\ (\Delta P/\mu u R_m)^b$ were tested on three sets of published data: one for CFMF of dried yeast suspensions in a laminar flow hollow fiber module, one for dried yeast suspensions in a turbulent flow tubular module and one for suspensions of latex particles in a laminar flow flat sheet module. The R^2 values for the fits of the correlations to the data were 0.98, 0.94, and 0.91 respectively.

Keywords: Crossflow microfiltration, dimensionless numbers, flux, correlation, steady state

INTRODUCTION

In the last two decades a large body of literature has appeared in the field of crossflow microfiltration (CFMF). Numerous papers have appeared in which researchers report experimental flux data for microbial and non-microbial suspensions. References (1–4) are just some recent examples that will direct the reader to earlier work and which illustrate the breadth of research in this area. In parallel with the experimental work, many mathematical models of

Received 5 January 2006, Accepted 9 May 2006
Address correspondence to Greg Foley, School of Biotechnology and National Institute for Cellular Biotechnology, Dublin City University, Dublin 9, Ireland. Tel.: +353-1-7005395; Fax: +353-1-7005412; E-mail: greg.foley@dcu.ie

CFMF have been developed and many of these have been reviewed by Davis (5). Some of these models provide good insight into the underlying physics of CFMF. For example, the force balance models are useful for interpreting phenomena such as preferential deposition of small particles (6, 7). The shear-induced diffusion model of Davis and co-workers (8–10) is probably the best known model of CFMF, and in addition to providing good insight into back-transport in crossflow systems, it agrees well with experiments performed with simple model systems composed of latex particle suspensions (11).

However, it is likely that approaches such as these will be unable to predict fluxes during crossflow microfiltration of complex microbial suspension encountered in real bioprocessing. Redkar and Davis (12) compared the predictions of the shear-induced diffusion model with data for crossflow microfiltration of suspensions of rehydrated bakers yeast and the study reveals some of the difficulties with trying to compare theoretical models with microbial system behaviour. Using one adjustable parameter (the "crossflow integral"), only moderate agreement was obtained between the model and the data. For a ceramic filter, the model overestimated the dependence of steady state flux on trans-membrane pressure and wall shear rate, while better agreement was obtained with a polypropylene filter. In the context of the pressure dependence, it is interesting to note that the model did not account explicitly for the pressure dependence of the specific resistance of yeast filter cakes (13). Regarding the weak dependence of flux on shear rate, it is worth pointing out that in the system studied, membrane fouling was clearly an important contributor to flux (although not included in the model), a fact that would weaken the dependence of the flux on crossflow velocity. In terms of the practical utility of the model, its one adjustable parameter was found to be a function of both the suspension *and the membrane* suggesting that the model must always be accompanied by experimentation for any given suspension-membrane system.

Further difficulties with applying theoretical models to CFMF of *microbial* suspensions can be anticipated when we consider the factors affecting the filtration characteristics of these suspensions. The specific resistance of microbial filter cakes, formed under dead-end conditions, depends not only on pressure, but also on factors such as cell morphology (14, 15) (which may change during fermentation), pH and ionic strength (16), surface properties (17), cell ageing (18) and harvest time (19), and these effects are not easily incorporated into mechanistic models. As an additional complication, the characteristics of the crossflow cake may depend on crossflow velocity due to preferential deposition of small cells (20) and alignment of cells parallel to the tangential flow (21) and may also be affected by membrane fouling (22).

At present therefore, it is reasonable that a more empirical approach be employed to correlate crossflow filtration behavior. Indeed, this is an

increasingly common approach as exemplified by the appearance of significant numbers of papers in which the use of artificial neural networks (ANNs) to correlate crossflow filtration data is reported (23–26). The ANN approach has proved to be a powerful technique for correlating data but provides very little insights into the underlying physics of a problem.

Dimensional analysis (27) is a technique that has found widespread use in the analysis of chemical engineering processes. Like artificial neural networks, it is used when physical phenomena are so complex that they cannot be described by predictive equations derived from first principles. Instead, dimensional analysis is used to reduce the number of variables in the problem, as a result of which, relatively simple empirical equations can be used to represent the experimental data. In contrast to neural networks, dimensional analysis can provide significant insight into the physics of a problem. CFMF is a complex process and would seem to be well suited to the dimensional analysis approach. Surprisingly, however, only a few attempts have been made to use dimensional analysis in crossflow microfiltration. Previous researchers have correlated CFMF data in terms of the cake resistance, the trans-membrane pressure, the crossflow velocity, and the suspension density (28–30). These approaches omitted key parameters such as the particle concentration.

In this paper we report on an attempt to correlate previously published CFMF data using a set of three dimensionless groups. The aim of the work is not to construct a correlation with wide applicability—the variability in microbial suspension and membrane properties precludes this—but to develop an approach whereby experimental data for a particular suspension-membrane system can be represented in a convenient and concise way. In the next section, we develop the relevant dimensionless groups. We then describe the process by which the raw data was obtained and the dimensionless groups calculated. Non-linear regression is then applied to obtain the relevant correlations.

DIMENSIONAL ANALYSIS OF CFMF

The number of variables that determine the steady state flux in CFMF is very large. Particle and liquid properties, process variables such as trans-membrane pressure and crossflow velocity, membrane properties, and module geometry are all significant. Inclusion of all of these variables would lead to a large number of dimensionless groups making data analysis very difficult. In this paper, we express the problem in the following way:

$$J = f\{\Delta P, u, c, R_m, \mu\} \tag{1}$$

where J is the steady state flux, ΔP is the trans-membrane pressure, u is the crossflow velocity, c is the particle concentration, μ is the filtrate viscosity,

and R_m is the membrane resistance. The membrane resistance is defined by the standard filtration equation,

$$J_{water} = \frac{\Delta P}{\mu R_m} \tag{2}$$

where J_{water} is the pure water flux through the membrane. Using the Buckingham Pi theorem, equation (1) implies that CFMF data can be correlated by three dimensionless groups (27). Applying the Buckingham Pi method gives

$$\frac{J}{u} = f\{\Pi_1, \Pi_2\} \tag{3}$$

where

$$\Pi_1 = \frac{\Delta P}{cu^2} \tag{4}$$

and

$$\Pi_2 = \frac{\Delta P}{\mu u R_m} \tag{5}$$

The physical significance of Π_1 is not obvious but it does have the familiar appearance of a friction factor, albeit with particle concentration replacing fluid density and trans-membrane pressure replacing wall shear stress. Π_2 is just the ratio J_0/u where J_0 is the initial flux.

DATA RETRIEVAL

There are many papers that probe the underlying mechanism of CFMF but these generally report selected data that test some aspect of a particular flux model (31–34). For this study we have used a paper that gives detailed steady state flux data for CFMF of re-hydrated bakers yeast suspensions (35) and a paper that gives comprehensive data on the CFMF of latex yeast suspensions (36). In the first paper (35) data were examined for two modules, characteristics of which are shown in Table 1. The raw data extracted from that paper are given in Tables 2 and 3. Where data was presented in graphical form in the original publication, the graphs were scanned, enlarged, and the data measured directly from the graph. In all calculations, the viscosity was taken to be 0.797×10^{-3}Ns/m^2 as all experiments were done at 30°C. In the

Table 1. Membrane and module characteristics in work of Patel et al. (35)

Module	Tube/fiber diameter	Membrane material	Membrane resistance
Tubular	5.5 mm	0.2 μm polypropylene	3.45×10^{11} m^{-1} ± 4%
Hollow fiber	1.1 mm	30 kDa polysulphone	1.79×10^{12} m^{-1} ± 15%

Table 2. Flux data for the hollow fiber module in the work of Patel et al. (35)

$c = 1$ g/L (dry weight)			$c = 3$ g/L (dry weight)			$c = 50$ g/L (dry weight)		
ΔP (kPa)	u (m/s)	J (m/s $\times 10^{-5}$)	ΔP (kPa)	u (m/s)	J (m/s $\times 10^{-5}$)	ΔP (kPa)	u (m/s)	J (m/s $\times 10^{-5}$)
28.2	0.5	1.59	43.2	1.0	1.70	34.5	1.0	0.56
38.8	1.0	1.90	56.5	1.0	1.87	103	0.5	1.48
47.6	1.0	2.08	68.8	1.5	2.03	103	1.0	1.69
49.4	0.5	2.16	77.6	0.5	2.23	103	1.5	1.36
68.8	1.5	2.62	79.4	1.0	2.28	125.8	1.0	1.67
79.4	0.5	2.96	89.1	1.5	2.45			
80.3	1.0	3.09	97.1	0.5	2.69			
82.1	1.8	3.01	98.8	1.8	2.72			
82.9	1.5	2.84	100.6	1.0	2.65			
96.2	1.5	3.02	100.6	1.5	2.75			
97.1	0.5	3.17	112.9	0.5	3.0			
103	1.0	3.19	113.8	1.8	2.95			
110.3	0.5	3.29	114.7	1.0	2.91			
111.2	1.0	3.21						

Table 3. Flux data for the tubular module in the work of Patel et al. (35)

$c = 1$ g/L (dry weight)			$c = 5$ g/L (dry weight)			$c = 50$ g/L (dry weight)		
ΔP (kPa)	u (m/s)	J (m/s × 10^{-5})	ΔP (kPa)	u (m/s)	J (m/s × 10^{-5})	ΔP (kPa)	u (m/s)	J (m/s × 10^{-5})
25.5	2.8	2.78	18.8	2.8	0.88	21.5	2.8	0.71
45.7	2.8	3.27	39.0	2.8	1.90	48.4	2.8	0.95
69.9	2.8	5.03	68.5	2.8	2.30	67.2	2.8	1.68
75.3	2.8	5.68	142.5	2.8	3.93	83.3	2.8	1.95
103.0	0.6	3.42	177.4	2.8	4.60	103	0.8	1.14
103.0	1.1	4.49	207.0	2.8	4.91	103	1.6	1.57
103.0	1.7	5.30	231.2	2.8	4.99	103	2.4	2.04
103.0	2.3	6.39				103	3.2	2.55
103.0	2.8	7.16				103	4.0	2.82
104.8	2.8	7.08				103.5	2.8	2.19
146.5	2.8	8.50				121.0	2.8	2.96
207.0	2.8	9.99				139.8	2.8	3.27
228.5	2.8	10.30				207.0	2.8	4.33
						219.1	2.8	4.41

second paper (36), data was retrieved for the microfiltration of 0.055 μm latex particles with a 30kDa PVDF membrane in a flat sheet module of channel height 0.98 mm with nominally laminar flow. All data was measured from graphs and is shown in Table 4. The runs in which the fluid viscosity was varied were performed by varying the temperature. It should be noted that the authors did not provide a value of R_m for their membrane and gave all concentrations in parts per million on a volume basis (ppmv). Thus our analysis did not evaluate the dimensionless constant, K, in equation (6) below but was capable of deriving the constants a and b.

RESULTS

Analysis of Yeast Microfiltration Data

We have assumed that the dimensionless steady state flux is a power-law function of the other dimensionless groups, i.e.

$$\frac{J}{u} = K\,\Pi_1^a\,\Pi_2^b \tag{6}$$

Table 4. Flux data for the 30 kDa membrane in the work of Hwang et al. (36)

ΔP (kPa)	u (m/s)	c (ppmv)	μ (Pa s × 10^{-3})	J (m/s × 10^{-4})
70	0.12	50	0.797	1.70
105	0.12	50	0.797	2.00
140	0.12	50	0.797	2.20
168	0.12	50	0.797	2.20
70	0.24	50	0.797	2.35
105	0.24	50	0.797	2.55
168	0.24	50	0.797	2.50
70	0.36	50	0.797	2.75
105	0.36	50	0.797	3.25
140	0.36	50	0.797	3.30
174	0.36	50	0.797	3.30
140	0.24	25	0.797	3.50
140	0.24	35	0.797	2.75
140	0.24	50	0.797	2.50
140	0.24	75	0.797	2.40
140	0.24	100	0.797	2.25
140	0.12	50	0.797	2.10
140	0.30	50	0.797	2.80
140	0.36	50	0.797	3.30
140	0.42	50	0.797	3.65
140	0.24	50	1.234	2.10
140	0.24	50	1.010	2.35
140	0.24	50	0.651	3.30

where K, a and b are dimensionless constants. The non-linear regression of the data was performed with SigmaPlot™ (SSI, California, USA) and we found the following expression for the hollow fiber data (Table 2)

$$\frac{J}{u} = 4.26 \times 10^{-4} \Pi_1^{0.21} \Pi_2^{0.52} \tag{7}$$

where this correlation is valid for the system studied only and where $650 < \Pi_1 < 4.2 \times 10^5$ and $2.4 \times 10^{-5} < \Pi_2 < 1.6 \times 10^{-4}$.

In the experiments with the hollow fiber membrane the *apparent* ratio of steady state cake resistance, R_c, to membrane resistance (i.e., assuming no membrane fouling) varied between 0.43 and 4.32, and 26 of the 32 experiments had an R_c/R_m ratio less than 2.0. The ratio was calculated in all cases by rearranging the filtration equation

$$J = \frac{\Delta P}{\mu(R_m + R_c)} \tag{8}$$

to give

$$\frac{R_c}{R_m} = \frac{\Delta P}{\mu R_m J} - 1 \tag{9}$$

where J is the measured steady state flux. Given the likelihood of membrane fouling occurring with the yeast suspensions employed (12), the true ratio of cake to membrane resistance was probably significantly lower than the values quoted above. Therefore in these experiments, the cake and membrane resistances were of the same order of magnitude and in many of the experiments, the membrane resistance dominated. This may in part explain why there is such a weak dependence of flux on crossflow velocity ($u^{0.06}$) contained in equation (7). The flux is most dependent on crossflow velocity when the cake resistance dominates. For example, the shear induced diffusion model predicts that the flux should be proportional to $u^{1.0}$ when the cake resistance is dominant (10). However, since the membrane resistance should be essentially independent of crossflow velocity, even if membrane fouling occurs, the observed dependence of the flux on crossflow velocity in real systems is determined by the relative magnitudes of the cake and membrane resistances. Thus, the very weak dependence of flux on crossflow velocity contained in equation (7) is reflective of the significance of the membrane resistance. Similarly the strong dependence on trans-membrane pressure ($\Delta P^{0.73}$) is indicative of the importance of membrane effects because for the compressible cakes formed in these experiments, the flux should be only very weakly dependent on the trans-membrane pressure when the cake resistance dominates but should be proportional to $\Delta P^{1.0}$ when the membrane resistance dominates. A simple model of crossflow microfiltration is outlined in the Appendix to support these arguments.

For the tubular module data (Table 3) we find:

$$\frac{J}{u} = 0.786\Pi_1^{0.25}\Pi_2^{0.15} \tag{10}$$

where this correlation is valid for $55 < \Pi_1 < 3.2 \times 10^5$ and $2.4 \times 10^{-5} < \Pi_2 < 6.6 \times 10^{-4}$. In the experiments with the tubular module, the apparent ratio of steady state cake resistance, R_c, to membrane resistance varied between 2.34 and 31.91, and 28 of the 34 experiments had an R_c/R_m ratio greater than 5.0. These higher R_c/R_m values are reflected in a stronger dependence of flux on crossflow velocity ($u^{0.35}$), a weaker dependence on pressure ($\Delta P^{0.4}$), and a weaker dependence of flux on membrane resistance ($R_m^{-0.15}$ as opposed to $R_m^{-0.52}$ for the hollow fiber module.) Of course, the stronger dependence of the flux on crossflow velocity is also indicative of the turbulent flow in the module as shown in the Appendix.

The fit of equations (7) and (10) to the data is shown in the parity plots, Figs. 1 and 2. The R^2 values for each of these plots are 0.98 and 0.94 respectively. It is clear that the dimensional analysis approach is capable of correlating a substantial amount of data into one simple relationship, for a particular membrane-suspension system. The increased scatter in the plot for the tubular module reflects the more scattered nature of the raw data (35) and does not, we believe, reflect a problem with applying this approach to turbulent flows.

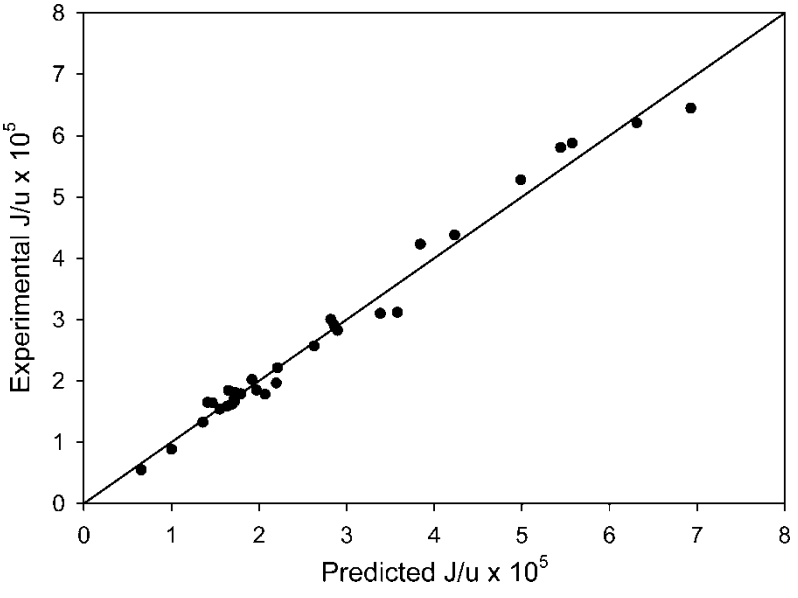

Figure 1. Experimental versus predicted values of J/u for CFMF of yeast suspensions in the hollow fibre module of Patel et al. (35).

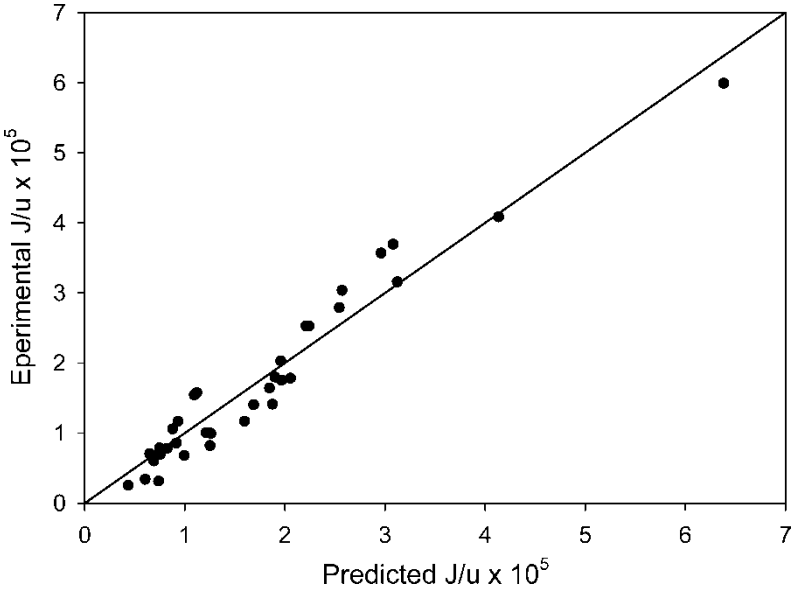

Figure 2. Experimental versus predicted values of J/u for CFMF of yeast suspensions in the tubular module of Patel et al. (35).

Analysis of Latex Microfiltration Data

The same approach was applied to the data of Hwang et al. (36) shown in Table 4. As mentioned above, the dimensionless constant, K, could not be obtained but the constants a and b were found by non-linear regression to be $a = 0.27$ and $b = 0.10$. The relevant parity plot is shown in Fig. 3 and indicates that this approach based on dimensionless numbers gives a moderately good fit ($R^2 = 0.91$) to the data, albeit not as good as that obtained with the yeast data. Whether this relatively poor fit in comparison with the yeast data reflects scatter in the original data of Hwang et al. (36), or whether it represents a weakness in applying this approach to the CFMF of such small particles is unclear at present. While the value of Π_2 is unknown in these calculations (due to the lack of information on R_m) the values of Π_1 ranged between 6900 and 2.5×10^5 which is within the ranges of the yeast studies described in the previous section. Although the flow in the latex experiments was nominally laminar, the exponents a and b obtained are quite close to those obtained with the turbulent flow yeast experiments. Interestingly, it would appear that in both these sets of experiments, the cake resistance is dominant. However, this conclusion must remain tentative because Hwang et al. (36) did not give R_m data and we have drawn this conclusion by inspection of their flux decline curves obtained at 140 kPa only, and assuming negligible membrane fouling as before. In addition, the importance

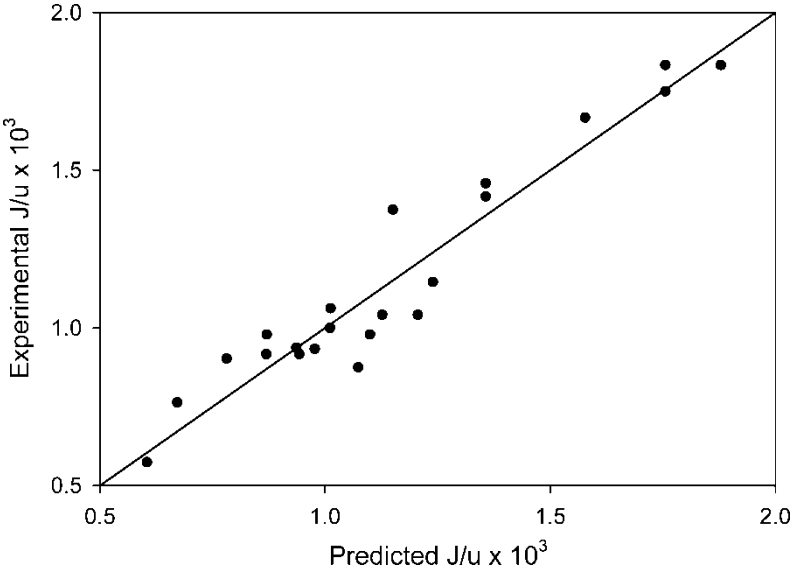

Figure 3. Experimental versus predicted values of J/u for CFMF of latex suspensions. Data of Hwang et al. (36).

of membrane fouling in each set of experiments remains unclear but one would expect it to be more significant in the yeast experiments.

DISCUSSION

The dimensional analysis approach appears to be a useful tool for correlating crossflow microfiltration data. In this paper we have shown that the results of large numbers of experiments obtained with a particular suspension-membrane system can be represented on a single graph and described by a single equation. Indeed it is perhaps surprising that this approach has not been applied more frequently in the past. Dimensional analysis has traditionally been applied to predict behavior in systems that are too complicated to analyse theoretically. CFMF is certainly a complex process particularly when real suspensions such as those encountered in bioprocessing are involved, and one would have thought that dimensional analysis would be an ideal approach for systems of this kind. There are two possible reasons for this. First, the number of parameters that can affect crossflow filtration behavior are potentially very large and the inclusion of all these parameters would lead to many dimensionless groups unless simplifications are made. In this study for example, we have not accounted *explicitly* for module geometry, crossflow regime, or suspension properties. This reduces the number of groups to a manageable level. As a consequence, the effect of

important industrial factors such as channel length are not revealed by the correlations developed here. Further experiments with membranes of various lengths would be needed to establish the effect of channel length on the constants, K, and possibly a and b, in the dimensionless correlations. Alternatively, an estimate of the effect of channel length could be made with, for example, the shear induced diffusion model (10).

A second reason why dimensional analysis has not been used extensively in crossflow microfiltration is that there have not been many systematic studies on the effect of process parameters on the steady state flux in crossflow microfiltration. While there are a large number of papers devoted to crossflow microfiltration processes as outlined earlier, few of these provide extensive information on the effect of process parameters on the steady state flux. Most authors have tried to provide insight into the underlying mechanism of CFMF and have focused on fundamental aspects of cake formation, membrane fouling, and flux dynamics. Thus, while it is very common to see plots of flux versus time in the typical crossflow filtration paper, it is very rare to find extensive tabular data showing the effect of process parameters on the flux at steady state. This makes it difficult for other researchers to get a quantitative overview of the factors affecting steady state fluxes.

The advantage of an experimental correlation like those developed here is that the flux behavior of a microfiltration system can be summarized concisely and accurately using an equation derived from a small number of experiments. Once a system is characterized in this way, its steady state flux under different conditions (e.g. of pressure, membrane resistance, concentration, and crossflow velocity) can be predicted. *A priori* prediction of the steady state flux from suspension properties, model geometry, and operating conditions is the long term goal of mathematical modelling approaches but in the medium term this is likely to be have limited success except with very well defined suspensions. The approach taken here, where we have merely tried to summarize process data in as concise a way as possible, is likely to be useful in the short to medium term.

While we have not attempted to generate a correlation that has wide ranging applicability in this paper, there is no reason why this approach could not be used for any kind of suspension, whether it be the incompressible latex suspensions or the moderately compressible yeast suspensions discussed in this paper, or highly compressible particles such as blood cells.

CONCLUSIONS

Crossflow microfiltration data for a particular suspension-membrane system can be represented with a single correlation involving three dimensionless groups. Apart from the fact that the data can be represented concisely, this finding may reduce the amount of experimentation required to characterize a given suspension-membrane system because only the relevant dimensionless

groups, and not the individual process parameters, need be varied. Further experimental work is required to test this approach in order to eliminate scatter produced by extracting data from graphs and to quantify precisely the starting membrane resistance in all experiments. A variety of suspension-membrane combinations should be used with a view to gaining insight into the factors affecting the exponents in the power-law correlations.

APPENDIX - A SIMPLE MODEL OF CROSSFLOW MICROFILTRATION

We assume that the process of cake build up is the net result of particle deposition and removal. Furthermore we assume that the removal is random and proportional to the cake mass per unit area giving

$$\frac{dm}{dt} = cJ - k\tau_w m \tag{A1}$$

The removal term used here owes its origins to the Kern-Seaton theory of heat transfer surface fouling (37) and has been used in a membrane context by a number of authors previously (38–40). At steady state and assuming

$$J = \frac{\Delta P}{\mu(R_m + \alpha m)} \tag{A2}$$

where α is the specific cake resistance, and that the cake is thin relative to the channel height, we get the following expression for the flux at steady state

$$J = \frac{2J_0}{1 + \sqrt{1 + F}} \tag{A3}$$

where J_0 is the initial flux and the dimensionless number, F, is given by

$$F = \frac{4\alpha c \Delta P}{\mu R_m^2 k\tau_w} \tag{A4}$$

At low pressures, we have $F \ll 1$ and the flux is proportional to the transmembrane pressure. At high pressures, the expression for the steady state reduces to

$$J = \left(\frac{k\tau_w \Delta P}{\alpha \mu c}\right)^{1/2} \tag{A5}$$

Assuming the specific cake resistance is related to pressure by the typical power-law expression

$$\alpha = a\Delta P^n \tag{A6}$$

where a and n are constants and typically $0 < n < 1$, we find that

$$J = \left(\frac{k\tau_w}{a\mu c}\right)^{1/2} \Delta P^{(1-n)/2} \tag{A7}$$

Thus, if n approaches 1.0, as it does for highly compressible cakes, the flux will be independent of pressure at high pressures. For incompressible cakes ($n = 0$) the exponent on the pressure dependence will be 0.5.

For laminar crossflow, the wall shear stress is proportional to the crossflow velocity and therefore this model predicts that the exponent on the velocity dependence varies from zero when the membrane resistance is dominant, to 0.5 when the cake resistance is dominant. For turbulent flow with constant friction factor, the velocity exponent varies between zero and 1.0. Therefore, the experimental dependence of flux on crossflow velocity is dependent on both the nature of the flow and the relative magnitudes of the cake and membrane resistances.

It should be pointed out that we have tested this model with the data given in Tables 2, 3 and 4 and did not find good agreement. Thus, its main use is in gaining a qualitative understanding of the effects of process parameters on the steady state flux.

NOMENCLATURE

a	empirical constant (−)
b	empirical constant (−)
c	cell concentration (g/L)
F	dimensionless number $= 4\alpha c\Delta P/\mu R_m^2 k \tau_w$
J	steady state flux (m/s)
J_0	initial flux (m/s)
k	cake removal constant (m^2/Ns)
K	empirical constant (−)
M	cake mass per unit area (kg/m^2)
n	empirical constant (−)
R_c	cake resistance (m^{-1})
R_m	membrane resistance (m^{-1})
u	crossflow velocity (m/s)

Greek Letters

α	specific cake resistance (m/kg)
ΔP	transmembrane pressure (N/m^2)
μ	filtrate viscosity (Ns/m^2)

Π_1	dimensionless number $= \Delta P/cu^2$
Π_2	dimensionless number $= \Delta P/\mu u R_m$
τ_w	wall shear stress (N/m^2)

REFERENCES

1. Keskinler, B., Yildiz, E., Erhan, E., Dogru, M., Bayhan, Y., and Akay, G. (2004) Crossflow microfiltration of low concentration-nonliving yeast suspensions. *J. Membr. Sci.*, 233: 59–69.
2. Mercier-Bonin, M. and Fonade, C. (2003) Enzyme transmission during crossflow filtration of yeast suspensions using gas/liquid two-phase flows. *Annals. New York Acad. Sci.*, 984: 480–491.
3. Xu, N., Zhao, Y., Zhong, J., and Shi, J. (2002) Crossflow microfiltration of micro-sized mineral suspensions using ceramic membranes. *Chem. Eng. Res. Des.*, 80 (A2): 215–222.
4. Sondhi, R. and Bhave, R. (2001) Role of backpulsing in fouling minimization in crossflow filtration with ceramic membranes. *J. Membr. Sci.*, 186: 41–52.
5. Davis, R.H. (1992) Modelling of fouling of crossflow filtration membranes. *Sep. Pur. Methods*, 21: 75–126.
6. Foley, G., Malone, D.M., and MacLoughlin, F. (1995) Modelling the effects of particle polydispersity in cross-flow filtration. *J. Membr. Sci.*, 99: 77–88.
7. Vyas, H.K., Bennett, R.J., and Marshall, A.D. (2001) Cake resistance and force balance mechanism in the crossflow microfiltration of lactalbumin particles. *J. Membr. Sci.*, 192: 165–176.
8. Romero, C.A. and Davis, R.H. (1988) Global model of cross-flow microfiltration based on hydrodynamic particle diffusion. *J. Membr. Sci.*, 39: 157–185.
9. Romero, C.A. and Davis, R.H. (1990) Transient model of cross-flow microfiltration. *Chem. Eng. Sci.*, 45: 13–25.
10. Davis, R.H. and Sherwood, J.D. (1990) A similarity solutions for steady state cross-flow microfiltration. *Chem. Eng. Sci.*, 45: 3203–3209.
11. Romero, C.A. and Davis, R.H. (1991) Experimental verification of the shear-induced hydrodynamic diffusion model of cross-flow microfiltration. *J. Membr. Sci.*, 62: 249–273.
12. Redkar, S.G. and Davis, R.H. (1993) Cross-flow microfiltration of yeast suspensions in tubular filters. *Biotechnol. Progr.*, 9: 625–634.
13. Meireles, A., Molle, C., Clifton, M.J., and Aimar, P. (2004) The origin of high hydraulic resistance for filter cakes of deformable particles: cell-bed deformation or surface-layer effect? *Chem. Eng. Sci.*, 59: 5819–5829.
14. McCarthy, A.A., Walsh, P.K., and Foley, G. (2002) Characterizing the packing and dead-end filter cake compressibility of the polymorphic yeast *Kluyveromyces marxianus* var. *marxianus NRRLy2415. J. Membr. Sci.*, 198: 87–94.
15. Oolman, T. and Liu, T.C. (1991) Filtration properties of mycelial microbial broths. *Biotechnol. Progr.*, 7: 534–539.
16. Ohmori, K. and Glatz, C.E. (1999) Effects of pH and ionic strength on microfiltration of *C. glutamicum*. *J. Membr. Sci.*, 153: 23–32.
17. Hodgson, P.H., Leslie, G.L., Schneider, R.P., Fane, A.G., Fell, C.J.D., and Marshall, K.C. (1993) Cake resistance and solute rejection in bacterial microfiltration- the role of the extracellular cell matrix. *J. Membr. Sci.*, 79: 35–53.

18. Meireles, M., Lavoute, E., and Bacchin, P. (2003) Filtration of a bacterial fermentation broth: harvest conditions effects on cake hydraulic resistance. Bioprocess. *Biosys. Eng.*, 25: 309–314.
19. Okamoto, Y., Ohmori, K., and Glatz, C.E. (2001) Harvest time effects on membrane cake resistance of *Escherichia coli* broths. *J. Membr. Sci.*, 190: 93–106.
20. Foley, G., MacLoughlin, P.F., and Malone, D.M. (1992) Preferential deposition of smaller cells during crossflow microfiltration of a yeast suspension. *Biotechnol. Tech.*, 6: 115–120.
21. Tanaka, T., Abe, K., Asakawa, H., Asaka, H., Yoshida, H., and Nakanishi, K. (1994) Filtration characteristics and structure of cake in cross-flow filtration of bacterial suspension. *J. Ferment. Bioeng.*, 78: 455–461.
22. McCarthy, A.A., Walsh, P.K., and Foley, G. (2002) Experimental techniques for measuring the cake mass, the cake and membrane resistances and the specific cake resistance during crossflow filtration of microbial cells. *J. Memb. Sci.*, 201: 31–45.
23. Piron, Latrille, E. and René, F. (1997) Application of artificial neural networks for crossflow microfiltration modelling: "black-box" and semi-physical approaches. *Computers in Chemical Engineering*, 2: 1021–1030.
24. Rai, P., Majumdar, G.C., DasGupta, S., and De, S. (2005) Modeling the performance of batch ultrafiltration of synthetic fruit juice and mosambi juice using artificial neural network. *J. Food Eng.*, 71: 273–281.
25. Aydiner, C., Demir, I., and Yildiz, E. (2005) Modeling of flux decline in crossflow microfiltration using neural networks: the case of phosphate removal. *J. Membr. Sci.*, 248: 53–62.
26. Chellam, S. (2005) Artificial neural network model for transient crossflow microfiltration of polydispersed suspensions. *J. Membr. Sci.*, 258: 35–42.
27. Geankoplis, C.J. (1983) *Transport Processes and Unit Operations*, 2nd Edition; Allyn and Bacon: Boston.
28. Asaadi, M. and White, D.A. (1992) A model for determining the steady state flux of inorganic microfiltration membranes. *Chem. Eng. J.*, 48: 11–16.
29. Elmaleh, S., Vera, L., Villarroel-Lopez, R., Abdelmoumni, L., Ghaffor, N., and Delgado, S. (1998) Dimensional analysis of steady state flux for microfiltration and ultrafiltration membranes. *J. Membr. Sci.*, 139: 37–45.
30. Gautam, S.K. and Pandya, R.V.R. (1997) Crossflow microfiltration of blood through an extracorporeal device: a study in parameterization. *Transfus. Sci.*, 18: 181–186.
31. Li, H., Fane, A.G., Coster, H.G.L., and Vigneswaran, S. (1998) Direct observation of particle deposition on the membrane surface during crossflow microfiltration. *J. Membr. Sci.*, 149: 83–97.
32. Altmann, J. and Ripperger, S. (1997) Particle deposition and layer formation at the crossflow microfiltration. *J. Membr. Sci.*, 124: 119–128.
33. Chellam, S. and Wiesner, M.R. (1998) Evaluation of crossflow filtration models based on shear-induced diffusion and particle adhesion: Complications induced by feed suspension polydispersivity. *J. Membr. Sci.*, 138: 83–97.
34. LeBerre, O. and Daufin, G. (1996) Skimmilk crossflow microfiltration performance versus permeation flux to wall shear stress ratio. *J. Membr. Sci.*, 117: 261–270.
35. Patel, P.N., Mehaia, M.A., and Cheryan, M. (1987) Cross-flow membrane filtration of yeast suspensions. *J. Biotechnol.*, 5: 1–16.
36. Hwang, S.J., Chang, D.J., and Chen, C.H. (1996) Steady state permeate flux for particle cross-flow filtration. *Chem. Eng. J. Biochem. Eng. J.*, 61: 171–178.

37. Kern, D.Q. and Seaton, R.E. (1959) A theoretical analysis of thermal surface fouling. *Brit. Chem. Eng.*, 4: 258–262.
38. Gutman, R.G. (1977) Design of membrane separation plant. 1. Design of RO modules. 2. Fouling of RO modules. *Chem. Eng.* (London), 322: 510–513, 521–523.
39. McCarthy, A., Walsh, P.K., and Foley, G. (1996) On the relation between filtrate flux and particle concentration in batch crossflow microfiltration. *Sep. Sci. Technol.*, 31: 1615–1627.
40. Silva, C.M., Reeve, D.W., Husain, H., Rabie, H.R., and Woodhouse, K.A. (2000) Model for flux prediction in high-shear microfiltration systems. *J. Membr. Sci.*, 173: 87–98.